Experimental Study of Load Carrying Capacity of Point Contacts at Zero Entrainment Velocity

B.A. Shogrin
Case Western Reserve University, Cleveland, Ohio

W.R. Jones, Jr.
Lewis Research Center, Cleveland, Ohio

E.P. Kingsbury
IRC, Walpole, Massachusetts

M.J. Jansen
AYT Corporation, Brook Park, Ohio

J.M. Prahl
Case Western Reserve University, Cleveland, Ohio

October 1998

Experimental Study of Load Carrying Capacity of Point Contacts at Zero Entrainment Velocity

B. A. Shogrin, W. R. Jones, Jr.[*], E. P. Kingsbury[**], M. J. Jansen[***], J. M. Prahl
Case Western Reserve University, Cleveland, Ohio, USA
[*]NASA Lewis Research Center, Cleveland, Ohio, USA
[**]IRC, Walpole, Massachusetts, USA
[***]AYT Corporation, Brookpark, Ohio, USA

SUMMARY

A capacitance technique was used to monitor the film thickness separating two steel balls while subjecting the ball-ball contact to highly stressed, zero entrainment velocity conditions. Tests were performed in a nitrogen atmosphere and utilized 52100 steel balls and a polyalphaolefin lubricant. Capacitance to film thickness accuracy was verified under pure rolling conditions using established EHL theory. Zero entrainment velocity tests were performed at sliding speeds from 6.0 to 10.0 m/s and for sustained amounts of time to 28.8 min. The protective lubricant film separating the specimens at zero entrainment velocity had a film thickness between 0.10 to 0.14 μm (4 to 6 μin), which corresponded to a λ value of 4. The formation of an immobile surface film formed by lubricant entrapment is discussed as an explanation of the load carrying capacity at zero entrainment velocity conditions, relevant to the ball-ball contacts occurring in retainerless ball bearings.

1 INTRODUCTION

Spacecraft use momentum and reaction wheels for attitude control. Three wheels are adequate, but redundant wheels are often included. Anomalies that have occurred on Skylab (1), INSAT I-D and Superbird have shown that these precautions are well founded. Torque and vibration anomalies can compromise performance.

Most failures and anomalies can be traced to the ball bearing retainers. Problems arise when the motion of the retainer becomes unstable. Instabilities are characterized by large, erratic increases in driving torque and large vibrations accompanying loud noise or squeal. Kingsbury (2, 3) concluded that driving torque increases to 300% can be attributed to retainer instabilities.

Retainers are usually made of a porous phenolic or polyimide material, which is saturated with lubricant by vacuum impregnation. Other than the original charge of free lubricant, the lubricant within the retainer is often the only supply available to the bearing during the 5 to 10 year life of the mechanism.

Research by Bertrand et al (4, 5) has shown that phenolic retainers, instead of supplying oil, actually absorb oil from the bearing. They have shown (4) that there is no net delivery of lubricant from a retainer to the metal parts, even in a well lubricated bearing having a fully-impregnated retainer, and demonstrated that damage can occur after the initial charge of lubricant begins to degrade.

Lubricant deprivation at the ball-retainer interface has been shown to cause retainer instability, leading to sporadic torque spikes, increased torque, and eventual bearing failure (2, 6, 7). Inconsistent lubricant flow from adjacent retainer pockets results in variable friction coefficients between the balls and pockets, which further fuels instabilities. Severe cases of lubricant deprivation at the pocket/ball interface result in pocket wear (7), which can lead to catastrophic bearing failure.

A solution to the crippling retainer-related bearing instability problems is to eliminate the retainer. Kingsbury (8) demonstrated that replacement retainerless bearing assemblies for failed control moment gyros of Skylab, operated without compromise in a 13,000 hour life test. However, retainerless bearing operation is often questioned because of the theoretical predictions of no load carrying capacity between neighboring bearing balls.

1.1 Theory

Skepticism surrounding retainerless bearings is well founded as the theoretical predictions of Hamrock and Dowson (9) for film thicknesses in fully flooded, isothermal EHL contacts are zero. In a retainerless bearing, the surface velocities of two neighboring balls at the point of contact are of the same magnitude but in opposite directions, and the entrainment velocity is zero, yielding the prediction of zero film thickness. This is echoed in the Reynold's equation. Since the entrainment velocity is zero, the pressure gradient along the direction of motion is also zero, and therefore, the load carrying capacity is zero.

1.2 Previous Zero Entrainment Velocity (ZEV) Research

There is evidence that a protective film is generated between two surfaces with equal and opposite peripheral velocities. Cameron (10) and Dyson and Wilson (11) demonstrated this phenomenon using line contacts. Cameron's tests utilized dissimilar metals in a disc machine. No scuffing occurred until a speed of 2.1 m/s and a maximum Hertzian stress (σ_{max}) of 0.44 GPa were reached. However, when two steel discs were run, scuffing occurred immediately. It was concluded that a thermal property mismatch was responsible and a "viscosity wedge" theory was proposed. Other researchers (13 to 15) from that era confirmed that steel discs scuffed at ZEV, even at very "light" loads.

However, Dyson and Wilson (11) demonstrated that two smooth steel surfaces at ZEV could support a σ_{max} of 0.7 GPa at speeds to 8 m/s. They suggested that failures reported by others were due to the rough surfaces of their steel discs.

Recently, there has been growing evidence of a protective film separating point contacts at ZEV. This comes from successful operation of retainerless bearings. This includes work by Kingsbury (8, 16 to 24), Hunter et al (25), Olsen (26), Schritz et al (27), DeLucie (28) and Jones et al (29, 30). This research represents thousands of hours of retainerless bearing operation without a single reported ball-ball failure.

In spite of this mountain of evidence, skepticism of load carrying capacity at ZEV still prevails. The most definitive way to determine the existence of load carrying capacity at ZEV is to isolate the contact from all other surroundings. This is the objective of this work.

2 EXPERIMENTAL APPARATUS

2.1 Tribometer

The tribometer used in this study is shown in Figure 1 and is described in detail in Reference 31 along with test procedures.
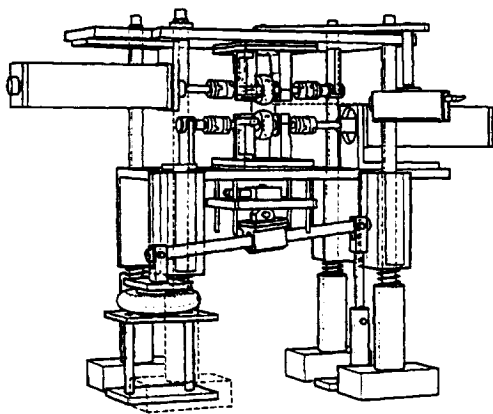
Figure 1 – Overall view of tribometer

The tribometer is mounted on a vibration isolation table and is enclosed in a plastic housing for atmosphere control. It is capable of subjecting its circular, point contact to a large array of EHL conditions. These include: rolling speeds to 10 m/s, contact stresses to 4 GPa, and any degree of slip.

The tribometer features two open faced spindle units with high running accuracy. Details are shown in Figure 2. Each spindle is driven by a servomotor with encoder feedback. Film
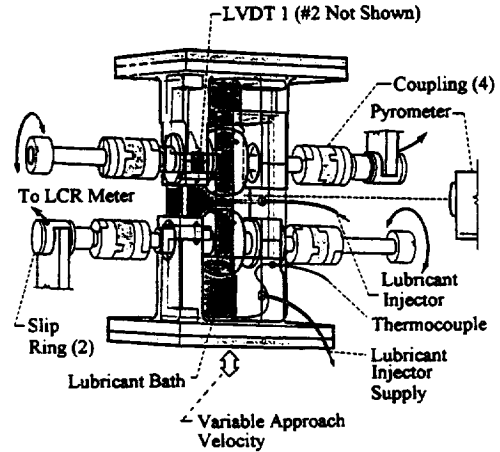
Figure 2 – Detailed view of specimens.

thickness is derived from capacitance measurements. A pneumatic system provides precise approach velocities and loading. Two LVDTs are used to measure the relative linear displacement of the lower spindle support and the distance between test specimens.

All tribometer functions are controlled with a LabVIEW-based, computer data acquisition (DAQ) system. This system automatically shuts down all operations and separates the specimens when user-defined limit criteria are exceeded, preventing damage to the specimens.

2.2 Test Specimens

The machined specimens were 0.064m (2.50 in) diameter AISI 52100 steel (Rockwell C 62) grade 100 bearing balls (R_a of 0.02 μm).

2.3 Capacitance Measurements

The capacitance and dissipation of the lubricating films were monitored with an HP4263A LCR meter with accuracy of $\pm$ 0.4% for capacitance and $\pm$ 0.004% for dissipation. Electrical connections to the rotating reference frame were made through mercury slip rings.

2.4 Loading System

Precise displacement of the lower support and contact is provided by a closed loop, pneumatic loading system. Ball-ball approach velocities and loading rates are as low as 12.5 nm/sec and 0.022 N/sec, respectively.

2.5 Lubricant

A filtered polyalphaolefin (PAO-182), fortified with an antiwear additive (tricresyl phosphate) and an antioxidant (hindered phenol) was used. A dielectric strength of 13.8 volts/cm was used. Effective pressure viscosity coefficients were determined by Smeeth et al (32). Lubricant was supplied to the contact by submerging the lower ball in a bath and also by injecting a stream of lubricant into the contact area. The bath and meniscus temperatures were monitored.

3 EXPERIMENTAL PROCEDURES

3.1 Specimen Preparation

Prior to spindle assembly, specimens were ultrasonically cleaned for 20 minutes in hexane, acetone and finally methanol. All tests were run with the same test specimens.

3.2 DAQ Limit Criteria

Resistance, dissipation factor and capacitance limit criteria were determined experimentally by statically loading specimens together and slowly separating (13.0 nm/sec) them while observing the LCR data of the lubricant formed around the contact. Typical minimum resistance limit criteria were set at 500 Ω and capacitance maximum at 25 pF. The maximum dissipation factor was 0.5. The maximum lubricant temperature was set at 35°C.

3.3 Pure Rolling Tests

The EHL film thickness was determined under pure rolling conditions. These results were compared to theoretical film thickness predictions to verify the capacitance-to-film thickness model.

3.4 Zero Entrainment Tests

These tests were initiated after qualifying the tribometer and film thickness approximation technique. Approach velocities ranged from 0.05 to 2.3 μm/sec. Tests at ZEV were separated into exploratory or conclusive. Exploratory tests were used to determine what approach velocities, failure limits and speeds to use for later tests. An important goal was to explore these conditions without contact failure. Therefore, initial tests were run under very conservative conditions. As experience was gained, the conditions necessary for sustained operation became evident. The conclusive tests were so named since they demonstrated that the contact could support a sustained load at ZEV without contact failure. A total of 25 tests were run at ZEV.

4 RESULTS

4.1 Capacitance To film Thickness Approximation

The capacitance to film thickness approximation is detailed elsewhere (31). The approach was first used by Dyson et al (33) for line contacts. A similar model was derived by Allen

et al (34) for elliptical contacts and used by Kingsbury et al (22) and Hunter et al (25).

4.2 Pure Rolling Tests

These tests were performed by bringing the motors to speed prior to contact, as the lower specimen approached the upper specimen. The approach and entrainment velocity (X 100) for test "3rwos" appear in Figure 3. The approach velocity was 2.68 μm/s. The motors were enabled at 2115 seconds, just
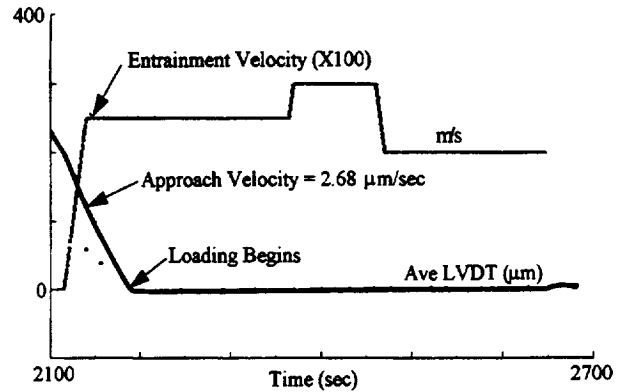
Figure 3 – Ball-ball approach and entrainment velocity (x100) for pure rolling test "3rwos"

prior to the onset of ball-ball loading. Loading began at 2190 seconds. A load rate of 0.45 N/s was used throughout the test. Contact stress began to increase to the desired stress of 0.62 · GPa at 2240 seconds. The entrainment velocity was first set to 2.5 m/s. After 200 seconds, it was increased to 3.0 m/s, where it remained for 100 seconds before being changed to 2.0 m/s.

Film thickness approximations appear in Figure 4, along with the theoretical minimum, h_{min}, and central film thickness, h_{cent},
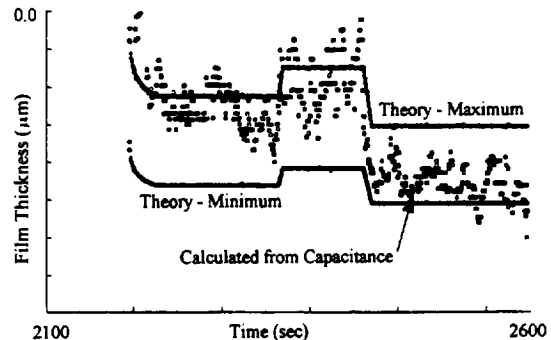
Figure 4 – Comparison between theoretical and experimental approximated film thickness for roll without slip test "3rwos"

calculations at 24°C using Hamrock and Dowson's equations (9). Both theoretical and approximated film thicknesses decreased as the two specimens began to load against one another at 2190 seconds at an entrainment velocity of 2.5 m/s. As the desired load was reached, all calculations leveled out until the entrainment velocity increased to 3.0 m/s at 2360 seconds. At 2460 seconds, the velocity was decreased to 2.0 m/s with an accompanying decrease in the calculated and

approximated film thicknesses. A total of five other sets of pure rolling tests were performed which verified the accuracy of the capacitance technique.

4.3 Zero Entrainment Velocity

A total of 25 tests were performed using ZEV. Nine of these tests violated limit criteria at the onset of ball-ball loading and were shutdown immediately. Nine other tests supported a small load for times ranging from 15 seconds to 9.6 minutes. Five tests demonstrated a sustained lubricant film under substantial load. The final two tests were performed at lower speeds (3.0 and 1.0 m/s). After each test, both surfaces were checked visually for damage, but none was observed. At the conclusion of all testing, one specimen was removed for analysis by optical microscopy.

Table 1 – ZEV test with load carrying capacity

Test #	Sliding Speed-m/s	Maximum Contact Stress -GPa	Duration min
22z	10.0	0.52	28.8
23z	8.0	0.57	28.2
21z	8.0	0.46	26.7
19z	6.0	0.35	17.5
20z	6.0	0.45	24.3

ZEV tests that demonstrated sustained load carrying capacity at elevated contact stresses are summarized in Table 1. Test "22z" sustained load for the longest time and was manually shutdown after 28.8 minutes at a σ_{max} of 0.52 GPa. The mean capacitance and calculated h_{film} were 21.8 pF and 0.143 µm, respectively.

The five test durations ranged from 17.5 to 28.8 minutes with σ_{max} from 0.35 to 0.57 GPa, and sliding velocities from 6.0 to 10.0 m/s. Two of these tests were manually terminated, after it was determined that they had shown adequate sustained load carrying capacity at ZEV. Two tests, "19z" and "23z," were shutdown due to IR temperature violations. Test "20z" was shutdown due to capacitance violations. Capacitance violations did not necessarily indicate metal to metal contact, but could have resulted from dielectric breakdown or electrical noise.

An important observation from these tests was that h_{film} is not affected by varying sliding velocity. Since the lubricant was not entrained into the contact, it is reasonable that a velocity dependence was not observed.

4.4 Graphical Representation Of ZEV Tests

The approach and load bearing portion of test "21z' as monitored by the LVDTs appear in Figure 5. During the approach, the voltage to the pneumatic loading system increased at a constant rate to reach the desired σ_{max}. Once the actual stress was within the desired range, loading ceased. A rise in contact temperature then caused additional loading. The actual and desired σ_{max} appear in Figure 6. This test was

manually terminated after 26.7 minutes. The calculated h_{min} corresponding to the smoothed capacitance appears in Figure 7. The h_{min} values were 0.14 µm ± 0.02 µm.
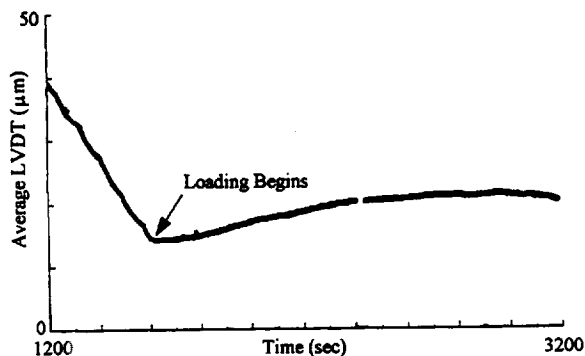
Figure 5 – Ball-ball final approach for zero entrainment velocity test "21z"
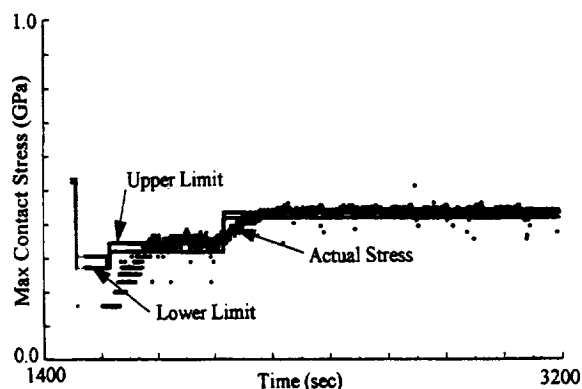
Figure 6 – Actual and desired maximum Hertzian contact stress for zero entrainment test "21z"
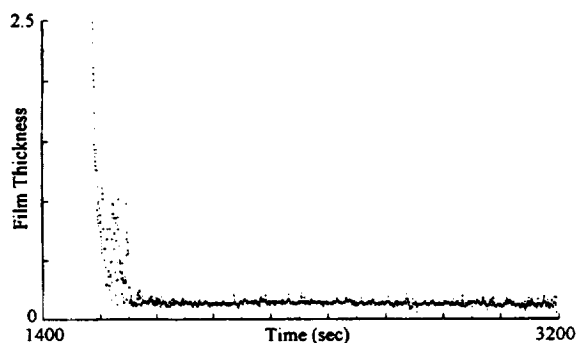
Figure 7 – Film thickness approximations for zero entrainment test "21z"

5 DISCUSSION

The success or failure of earlier experiments (10, 11, 13 to 15) involving disc machines under ZEV strongly depended upon

4

specimen surface finish. The first report of load carrying capacity of a point contact at ZEV was performed by Kingsbury (17). This was demonstrated with a 440C retainerless bearing operating at 1 GPa with three different lubricants.

Kingsbury's work was taken further by Olson (26) and DeLucie (28). Similar rigs were used with 52100 steel specimens and a variety of lubricants. Ball-ball contact stresses to 1 GPa were obtained at sliding speeds to 25.5 m/s.

5.1 Boundary Film Phenomena

The demonstrated load carrying capacity at ZEV is considered to be a boundary film phenomenon. Standard EHL theories are not equipped to model such films. Although, a definitive explanation for this surface protection is still sought, there are plausible arguments. Recent work (32) in ultrathin film EHL has indicated the presence of tenacious, immobile films at low rolling speeds. Additionally, it is plausible that the reactive film produced by the TCP additive contributes to the protection.

5.2 Thick Immobile Layers

Earlier work (35 to 37) indirectly demonstrated the presence of adsorbed, multimolecular films whose properties differed from that of the bulk fluid. Immobile layers were demonstrated by Fuks (37) as he showed that two loaded parallel steel discs submerged in mineral oil remained separated by a thin layer of oil after several hours under load.

More recently, Georges et al (38) detected immobile films approx. two to ten molecular layers thick in static squeeze film tests. These films were said not to participate in the hydrodynamic fluid flow and were detected on all substrates tested. Of course, these experiments were at low contact stress and without relative motion.

Recent studies (32, 39) have used ultrathin film interferometry to investigate immobile films in EHL. Smeeth et al (32) detected immobile surface films to 20 nm thick at rolling speeds to 0.1 m/s and σ_{max} to 0.52 GPa with various polymer blends. These films had much higher viscosities than the bulk lubricant. These films had a thickness independent of entrainment velocity and slowly squeezed out of the contact once motion ceased (39). As speeds increased, a conventional EHL film was produced which was superimposed on the immobile film. Immobile film formation was independent of temperature.

Since these layers slowly squeezed out after motion had stopped, Cann and Spikes (39) postulated that the rolling motion trapped these films, which could not be displaced by viscous flow within the time it took the contact to confine it. After rolling ceased, there was ample time for the polymers to untangle and flow from the contact. This suggested a time factor in immobile film formation.

The work here suggests that there is a speed/stress relationship corresponding to a critical entrapped, immobile

boundary film that is capable of sustaining a load. As the sliding speed was decreased to 1 m/s, the load the film could support also decreased.

6   SUMMARY

A unique test facility was used to determine the existence and magnitude of a lubricating film at a point contact subjected to zero entrainment velocity and high stresses.

Despite contrary theoretical predictions, substantial, sustained load carrying capacities were demonstrated at zero entrainment velocity without surface damage. σ_{max} to 0.57 GPa were supported at sliding speeds to 10.0 m/s for sustained periods of time.

7   CONCLUSION

The observed lubricating ability and load carrying capacity at zero entrainment velocity is considered to be a boundary layer phenomenon caused by the formation of an entrapped immobile surface film.

8   REFERENCES

1. "Proceeding of the Committee to Investigate the Skylab CMG No. 2 Orbital Anomalies," Marshall Space Flight Center, (Jan. 1974).
2. Kingsbury, E., "Torque Variations in Instrument Ball Bearings," ASLE Trans., 8, (1965), 435-441.
3. Kingsbury, E. And Walker, R., "Motions of an Unstable Retainer in an Instrument Ball Bearing," J. of Trib., 116, (Apr. 1994), 202-208.
4. Bertrand, P.A., Carre, D.J. and Bauer, R., "Oil Exchange Between Ball Bearings and Cotton-Phenolic Ball Bearing Retainers," Trib. Trans., 38, 2, (1995), 342-352.
5. Bertrand, P.A., "Oil Absorption into Cotton-Phenolic Material," J. Mater. Res., 8, 7, (July 1993), 1749-1757.
6. Loewenthal, S., Boesinger, E.A. and Donley, A.D., "Observations of Cage Instability," Proc. Of DOD/Instrument Bearing Working Group, (1991).
7. Gupta, P.K., "Frictional Instabilities in Ball Bearings," Trib. Trans., 31, 2, (1988), 258-268.
8. Kingsbury, E., "Large Bearing Operation Without Retainer," Lubr. Engr., 35, 9, (1979), 517-520.
9. Hamrock, B.J. and Dowson, D., Ball Bearing Lubrication. The Elastohydrodynamics of Elliptical Contacts, John Wiley & Sons, Inc., (1981).
10. Cameron, A., "Hydrodynamic Lubrication of Rotating Disks in Pure Sliding. A new Type of Oil Film Formation," J. Inst. Of Petrol., 37, (1951), 471-486.
11. Dyson, A. And Wilson, A.R., "Film Thickness in Elastohydrodynamic Lubrication at High slide/Roll Ratios," Proc. Inst. Mech. Engr., 183, (1968-69), 81-97.
12. Cameron, A., "The Viscosity Wedge," ASLE Trans., 1, (1958), 248.
13. Merritt, H.E., "Worm Gear Performance," Proc. Inst. Mech Engr., 128, (1935), 127.
14. Misharin, Y.A. and Sivyakova, A.V., "A Laboratory Study of Anti-seizur3 Properties of Certain Materials

5

Used for Worm Gears," Nat. Res. Council of Canada, Tech. Trans., TT-1058, (1963).

15. Blok, H., "Gear Wear as Related to Viscosity of Oil," Mech. Wear, Proc. Conf. MIT, Cambridge, MA, (June 1948).

16. Kingsbury, E.P., "Lubricant-Breakdown in Instrument Ball Bearings," J. of Lub. Tech., **100**, (July 1978), 386-394.

17. Kingsbury, E.P., "Ball-Ball Load Carrying Capacity in Retainerless Angular-Contact Bearings," J. of Lub. Tech., **104**, (1982), 327-329.

18. Kingsbury, E.P., "Influences on Polymer Formation Rate in Instrument Ball Bearings," Trib. Trans., **35**, 1, (1992), 184-188.

19. Kingsbury, E.P., "Basic Speed Ratio of an Angular Contact Bearing," J. of Lub. Tech., **102**, (July 1980), 391-394.

20. Kingsbury, E.P., "Slip Measurement in an Angular Contact Ball Bearing," J. of Lub. Tech., **105**, (April 1983), 162-165.

21. Kingsbury, E.P., "Dynamic and Coupling Influences on Basic Speed Ratio of an Angular Contact Bearing," Wear, **63**, (1980), 189-196.

22. Kingsbury, e., Schritz, B. and Prahl, J., "Parched Elastohydrodynamic Lubrication Film Thickness Measurement in an Instrument Ball Bearing," Trib. Trans., **33**, 1, (1990), 11-14.

23. Kingsbury, E.P., "Ball Contact Locus in an Angular Contact Bearing," J. Lub. Tech., **105**, 2, (1983), 166-170.

24. Kingsbury, E.P., "Ball Motion Perturbation in an Angular Contact Ball Bearing," ASLE Trans., **25**, (1982), 279-282.

25. Hunter, S., Kingsbury, E. And Prahl, J., "Oil Film Thickness and Analysis for an Angular Contact Ball Bearing Operating in Parched Elastohydrodynamic Lubrication," Proc. Inst. Mech. Eng. (London), Tribology-Friction, Lubrication and Wear, **I**, (1987), 81-84.

26. Olsen, A.J., "Load Carrying Capacity Between Lubricated Counter rotating Balls," Masters of Science Thesis, Mass. Inst. Of Tech., (1990).

27. Schritz, B. Jones, W.R., Jr., Prahl, J. and Jansen, R., "Parched Elastohydrodynamic Lubrication: Instrumentation and Procedure," Trib. Trans., **37**, 1, (1994), 13-22.

28. DeLucie, D., "Load Carrying Capacity of counter Rotating Balls in a retainerless Bearing," Masters of Science Thesis, Mass. Inst. of Tech., (1992).

29. Jones, W.R., Jr., Shogrin, B.A. and Kingsbury, E.P., "Long Term Performance of a Retainerless Bearing Cartridge With an Oozing Flow Lubricator for Spacecraft Applications," NASA TM 107492 (1997).

30. Jones,, W.R., Jr., Toddy, T.J., Predmore, R., Shogrin, B. and Herrera-Fierro, P., "The Effect of ODC-Free Cleaning Techniques on Bearing Lifetimes in the Parched Elastohydrodynamic Regime," NASA TM 107322, (1996).

31. Shogrin, B.A., "Experimental Determination of Load Carrying Capacity of Point Contacts at Zero Entrainment Velocity, Ph.D. Dissertation, Case-Western Reserve Univ., Cleveland, OH, (1998).

32. Smeeth, M., Spikes, H.A. and Gunsel, S., "The Formation of Viscous Surface Films by Polymer Solutions: Boundary or Elastohydrodynamic Lubrication," Trib. Trans., **39**, 3, (1996), 720-725.

33. Dyson, A., Naylor, H. And Wilson, A.R., "The Measurement of Oil-Film Thickness in Elastohydrodynamic Contacts," Proc. Instn. Mech. Engrs., Part 3B, **180**, (1965-66), 119-134.

34. Allen, G.E., Peacock, L.A. and Rhoads, W.L., "Measurement of Lubricant Film Thickness in Hertzian Contacts," NASA CR 105378, (1968).

35. Allen, C.M. and Drauglis, E., "Boundary Layer Lubrication: Minelayer or Multilayer," Wear, **14**, (1969), 363-384.

36. Needs, S.J., "Boundary Film Investigations," Trans. ASME, **62**, (1940), 331.

37. Fuks, G.I., "The Properties of Solutions of Organic Solids in Liquid Hydrocarbons at Solid Surfaces," in B.V. Deryagin (ed), Research in Surface Forces, **1**, (1960).

38. Georges, J.M., Millot, S., Loubet, J.L. and Tonck, A., "Drainage of Thin Liquid Films Between Relatively Smooth surfaces," J. Chem. Phys., **98**, 9, (1993).

39. Cann, P.M. and Spikes, H.A., "The Behavior of Polymer Solutions in Concentrated Contacts: Immobile Surface Layer Formation," Trib. Trans., **37**, 3, (1994), 580-586.

REPORT DOCUMENTATION PAGE

1. AGENCY USE ONLY (Leave blank)	2. REPORT DATE October 1998	3. REPORT TYPE AND DATES COVERED Technical Memorandum

4. TITLE AND SUBTITLE

Experimental Study of Load Carrying Capacity of Point Contacts at Zero Entrainment Velocity

5. FUNDING NUMBERS

WU–274–00–00–00

6. AUTHOR(S)

B.A. Shogrin, W.R. Jones, Jr., E.P. Kingsbury, M.J. Jansen, and J.M. Prahl

7. PERFORMING ORGANIZATION NAME(S) AND ADDRESS(ES)

National Aeronautics and Space Administration
Lewis Research Center
Cleveland, Ohio 44135–3191

8. PERFORMING ORGANIZATION REPORT NUMBER

E–11369

9. SPONSORING/MONITORING AGENCY NAME(S) AND ADDRESS(ES)

National Aeronautics and Space Administration
Washington, DC 20546–0001

10. SPONSORING/MONITORING AGENCY REPORT NUMBER

NASA TM—1998-208650

11. SUPPLEMENTARY NOTES

12a. DISTRIBUTION/AVAILABILITY STATEMENT

Unclassified - Unlimited
Subject Category: 34   Distribution: Nonstandard

This publication is available from the NASA Center for AeroSpace Information, (301) 621–0390.

12b. DISTRIBUTION CODE

13. ABSTRACT (Maximum 200 words)

A capacitance technique was used to monitor the film thickness separating two steel balls while subjecting the ball-ball contact to highly stressed, zero entrainment velocity conditions. Tests were performed in a nitrogen atmosphere and utilized 52100 steel balls and a polyalphaolefin lubricant. Capacitance to film thickness accuracy was verified under pure rolling conditions using established EHL theory. Zero entrainment velocity tests were performed at sliding speeds from 6.0 to 10.0 m/s and for sustained amounts of time to 28.8 min. The protective lubricant film separating the specimens at zero entrainment velocity had a film thickness between 0.10 to 0.14 μm (4 to 6 μin.), which corresponded to a λ value of 4. The formation of an immobile surface film formed by lubricant entrapment is discussed as an explanation of the load carrying capacity at zero entrainment velocity conditions, relevant to the ball-ball contacts occurring in retainerless ball bearings.

14. SUBJECT TERMS

Tribology; Retainerless bearings

15. NUMBER OF PAGES
12

16. PRICE CODE
A03

17. SECURITY CLASSIFICATION OF REPORT Unclassified	18. SECURITY CLASSIFICATION OF THIS PAGE Unclassified	19. SECURITY CLASSIFICATION OF ABSTRACT Unclassified	20. LIMITATION OF ABSTRACT